ORIGINAL ARTICLE

Anther cones increase pollen release in buzz-pollinated *Solanum* flowers

Mario Vallejo-Marín,[1,2,3] **Carlos Eduardo Pereira Nunes,**[1] **and Avery Leigh Russell**[2]

[1]*Biological and Environmental Sciences, University of Stirling, Stirling FK9 4LA, United Kingdom*

[2]*Department of Biology, Missouri State University, Springfield, Missouri 65897*

[3]*E-mail: mario.vallejo@stir.ac.uk*

The widespread evolution of tube-like anthers releasing pollen from apical pores is associated with buzz pollination, in which bees vibrate flowers to remove pollen. The mechanical connection among anthers in buzz-pollinated species varies from loosely held conformations, to anthers tightly held together with trichomes or bioadhesives forming a functionally joined conical structure (anther cone). Joined anther cones in buzz-pollinated species have evolved independently across plant families and via different genetic mechanisms, yet their functional significance remains mostly untested. We used experimental manipulations to compare vibrational and functional (pollen release) consequences of joined anther cones in three buzz-pollinated species of *Solanum* (Solanaceae). We applied bee-like vibrations to focal anthers in flowers with ("joined") and without ("free") experimentally created joined anther cones, and characterized vibrations transmitted to other anthers and the amount of pollen released. We found that joined anther architectures cause nonfocal anthers to vibrate at higher amplitudes than free architectures. Moreover, in the two species with naturally loosely held anthers, anther fusion increases pollen release, whereas in the species with a free but naturally compact architecture it does not. We discuss hypotheses for the adaptive significance of the convergent evolution of joined anther cones.

KEY WORDS: Anther cone, bees, buzz pollination, convergent evolution, pollen release, pollination.

Flowers are extremely morphologically diverse, and establishing how this morphological diversity affects function has long been a focus of research (Darwin 1877; Vogel 1996). Buzz-pollinated plants capture the close relationship between floral form and function. In these species, modifications of floral structures result in morphologies that require the visits of bees that produce vibrations to remove pollen grains (Macior 1968; Thorp and Estes 1975; Buchmann et al. 1977). The floral vibrations produced by the bee cause the anthers to shake, transmitting energy to the pollen grains inside the anthers and causing them to be propelled outward through the apical pores (Buchmann and Hurley 1978). In buzz-pollinated plants, floral structures, usually the anthers, but sometimes the corolla, have evolved a tubular form that retains the pollen grains inside after anthesis (Buchmann 1983; Vallejo-Marín 2019). A taxonomically widespread floral form of buzz-pollinated plants that has evolved convergently across multiple plant families is the *Solanum*-like

or "solanoid" flower, named by Fægri (1986) after the canonical flower form of *Solanum* (Solanaceae) (Endress 1996a; De Luca and Vallejo-Marin 2013; Russell et al. 2016). In *Solanum*-like flowers, the anthers are often arranged in the center of the flower forming a structure that resembles a cone (Faegri 1986). The degree to which the anthers in the solanoid flower are physically connected to one another varies. In one extreme, the enlarged stamens might be held loosely toward the center of the flower, with each individual stamen capable of relatively independent movement from the other stamens ("free" stamen architecture). Other species may have connivent anthers that are closely pressed together yet nonjoined. In the other extreme, anthers can be physically attached to each other (postgenitally connate; Endress 1996a), forming a single conical structure (Glover et al. 2004). This type of joined anther cone ("joined" architecture) has evolved multiple independent times in different plant groups including species in the families Anthericaceae,

Ehretiaceae, Luzuriageaceae, Pittosporaceae, Tecophilaceae, and Solanaceae (Glover et al. 2004; Holstein and Gottschling 2018; Endress 1996a). Despite the repeated evolution of conical anther architecture across different species, to date, no studies have tried to empirically evaluate its functional significance.

During buzz pollination, an individual bee might only vibrate one or few anthers. However, the vibrations generated by the bee's thorax and applied to this focal anther(s) propagate through the flower (Brito et al. 2020; Nevard et al. 2021), and can cause pollen release even in distal anthers that are not in direct contact with the bee's body (Arroyo-Correa et al. 2019). These oscillations in the focal anther(s) can cause other stamens to vibrate via two transmission pathways: (1) Filament pathway. Anthers are attached to the corolla or to the base of the flower via a filament that, in buzz-pollinated plants, is usually short and relatively stiff. The oscillation of the focal anther can thus cause shaking in the whole flower via the filament attachment, which in turn causes vibrations in other, nonfocal anthers. (2) Anther–anther pathway. In species with floral architectures in which stamens are held closely together, for example, forming a cone (joined anthers) (Glover et al. 2004), vibrations can be transmitted by direct anther–anther contact from the vibrating focal anther to adjacent anthers even when these distal anthers are not touching the bee's body. Recent work across buzz-pollinated flowers with different morphologies in three different plant families (Solanaceae, Primulaceae, and Gentianaceae) suggests that stamen architecture—defined as the stamen's relative sizes, degree of fusion, and their spatial and functional connections (Endress 1996b)—affects the transmission of vibrations (Nevard et al. 2021). Therefore, variation in stamen architecture could be associated with different types of vibrations experienced by distal, nonfocal anthers during buzz pollination with potential consequences for pollen release and pollen placement on the pollinator's body (Glover et al. 2004; Nevard et al. 2021).

Here, we use an experimental approach to compare the vibrational and functional (pollen release) consequences of joined anther cones in buzz-pollinated species in the genus *Solanum* (Solanaceae). Specifically, we address the following two questions: (1) How do the vibrations experienced in stamens differ between floral configurations with free versus joined anthers? We hypothesize that when vibrations are applied to a focal anther (proximate anther), the vibration amplitude experienced by distal anthers (those anthers not directly being vibrated) is higher in floral configurations with joined anthers than in floral configurations with free anthers. Our hypothesis assumes that species with loose anthers mainly transmit vibrations to distal anthers via the filament pathway, whereas anther fusion enables vibration transmission via both the filament and anther–anther pathways. (2) How does anther fusion into a cone affect pollen release upon vibrations? We hypothesize that the higher vibration amplitude

of anthers in joined architectures result in higher pollen release compared to free anther configurations. Our hypothesis is based on the fact that higher vibration amplitudes (e.g., higher velocity or acceleration amplitude) have been shown to be theoretically (Buchmann and Hurley 1978; Hansen et al. 2021) and empirically associated with higher rates of pollen release (De Luca et al. 2013; Rosi-Denadai et al. 2020; Kemp and Vallejo-Marin 2021). If joined anther architectures are associated with higher vibration magnitudes across more anthers (both focal and distal anthers), then we would expect pollen release to be proportionally higher as well.

Material and Methods
STUDY SYSTEM

Solanum L. is the largest buzz-pollinated genus of flowering plants with approximately 1400 species (Knapp 2002; Sarkinen et al. 2013). Within the genus *Solanum* and its close relatives, phylogenetic examination reveals that joined anther cones have evolved multiple times and represent a striking example of convergent evolution (Glover et al. 2004; Davis 2019). Joined anther cones have evolved independently across different clades of *Solanum* and relatives in at least four separate occasions: in tomatoes (*S. lycopersicum* L., sect. *Lycopersicon*) and its wild relatives, in *S. dulcamara* L. (sect. *Dulcamara*), in *S. luridifuscescens* Bitter (sect. *Cyphomandropsis*) and related taxa (Glover et al. 2004; Falcão et al. 2016), and in some species of *Lycianthes* such as *L. synanthera* and *L. anomala* (Dean et al. 2020). Strikingly, the joined anther cone in clades of *Solanum* is formed via different attachment mechanisms. In *S. lycopersicum* and *S. luridifuscescens*, the anther cone is formed via interlocking epidermal cells, joining adjacent anthers, whereas in *S. dulcamara* smooth anthers are held together by adhesive secretions (Glover et al. 2004; Falcão et al. 2016). In some cases, the pores of individual anthers in species with joined cones can secondarily evolve increasingly longitudinally dehiscent slits as in *S. lycopersicum* and related taxa. In these species, the slits open to the interior of the joined cone that functions as a single poricidal unit (Endress 1996a).

We studied three *Solanum* species from the subgenus *Leptostemonum* that differ in stamen architecture, specifically, the extent to which the anthers are loosely or closely held together: *Solanum sisymbriifolium* Lam. and *S. elaeagnifolium* Cav. have free, relatively loose, stamen architectures, whereas *S. pyracanthos* Lam. has stamens that, although not joined, are held closely together forming a cone-like structure. In *S. sisymbriifolium* and *S. elaeagnifolium*, the petals become reflexed soon after anthesis, and the anthers, which are loosely connivent at anthesis, become increasingly spread out (Knapp 2014a; Vorontsova and Knapp 2014). In *S. pyracanthos*, the petals are slightly reflexed, and the

Figure 1. Flower profiles of the three studied species of *Solanum* before (left-hand side panels) and after (right-hand side panels) applying the experimental treatment joining the anthers in a joined cone. The left hand-side panels show the flowers in their natural form and orientation. Notice the natural variation in the level of contact between the individual anthers across the three species, with *S. sisymbriifolium* and *S. elaeagnifolium* having relatively free anthers, whereas the anthers of *S. pyracanthos* are naturally arranged in a connivent cone. (a, b) *S. sisymbriifolium*; (c, d) *S. elaeagnifolium*; (e, f) *S. pyracanthos*. Scale bar = 1 cm.

stamens are free but held closely together forming a conical structure that persists throughout anthesis. All three species are nectarless, andromonoecious (producing both hermaphroditic and staminate flowers in the same individual) (Knapp 2014a; D'Arcy 1992; Vorontsova and Knapp 2014), and present flowers to pollinators more or less horizontally, with the anthers' long axis pointing parallel to the ground (Fig. 1). We used seeds of two accessions of *S. sisymbriifolium*, either from seeds collected in the field and outcrossed in the glasshouse or sourced from a commercial provider (Chiltern Seeds, Wallingford, UK) (Table 1). For *S. elaeagnifolium*, we used two accessions of this species collected in arid regions in Mexico where they formed locally abundant populations along roadsides and train tracks (Table 1). A summary of the distribution, floral characteristics, and floral visitors of these species as well as the accessions used in this study is presented in Table 1.

PLANT GROWTH

Seeds were germinated following a 24-h treatment with 1000 ppm aqueous solution of gibberellic acid (GA3, Asklepios-seeds, Bad Liebenzell, Germany) at room temperature. Approximately 10 days after germination, seedlings were transplanted to 1.5-L plastic pots with an 80:20 compost mix of John Innes No. 2 and medium grade perlite (LBS Horticulture, Colne, UK), and placed in a Snijders Microclimate cabinet in the Controlled Environment Facilities at the University of Stirling with the following growth conditions: 16 h light/8 h dark cycles, at 27°C/25°C, with constant 50% relative humidity. A few additional plants of *S. pyracanthos* and *S. elaeagnifolium* were transplanted to 10-L pots and placed in the glasshouse with 16 h of supplemental light using compact fluorescent lamps and provided with heating to keep temperature above 16°C at night. Plants were fertilized

Table 1. Species distribution, flower and anther characteristics, floral visitors, and accessions of the three *Solanum* species used in the present study. Accessions 1179F and 1180M were sourced commercially (see *Methods*) and their exact origin is unknown.

Species	Native Range	Corolla Diameter (Anther Length × Width) mm / Anther Size	Floral Visitors	Accession	Population	Lat.	Lon.	References
S. elaeagnifolium	Americas	20–35 (6–10 × 1.5–2)	*Amegilla, Bombus, Centris, Exomalopsis, Melissodes, Nomia, Protandrena, Pseudapis, Ptiloglossa, Xylocopa*	10-QSJ-12	Querétaro, México	20.37	99.99	Buchmann and Cane 1989; Tscheulin et al. 2009; Knapp 2014a; Petanidou et al. 2018
				11s36	Puebla, México	18.46	97.40	
S. pyracanthos	Madagascar	23–30 (6–7 × 1.5–2)	Unknown, but likely to include Malagasy *Nomia* and *Xylocopa*	1179F	Unknown	–	–	Armbruster et al. 2013; Knapp 2014b; Plebani et al. 2015
S. sisymbriifolium	South America	20–35 (9–10 × 1.5–2)	*Parapsaenythia* sp., *Augochlora* spp., *Augochloropsis* spp., *Dialictus* sp., *Xylocopa* sp.	F1-sys-3	Salta, Argentina	–24.71	–65.41	Vorontsova and Knapp 2014; Ramos et al. 2016
				1180M	Unknown	–	–	
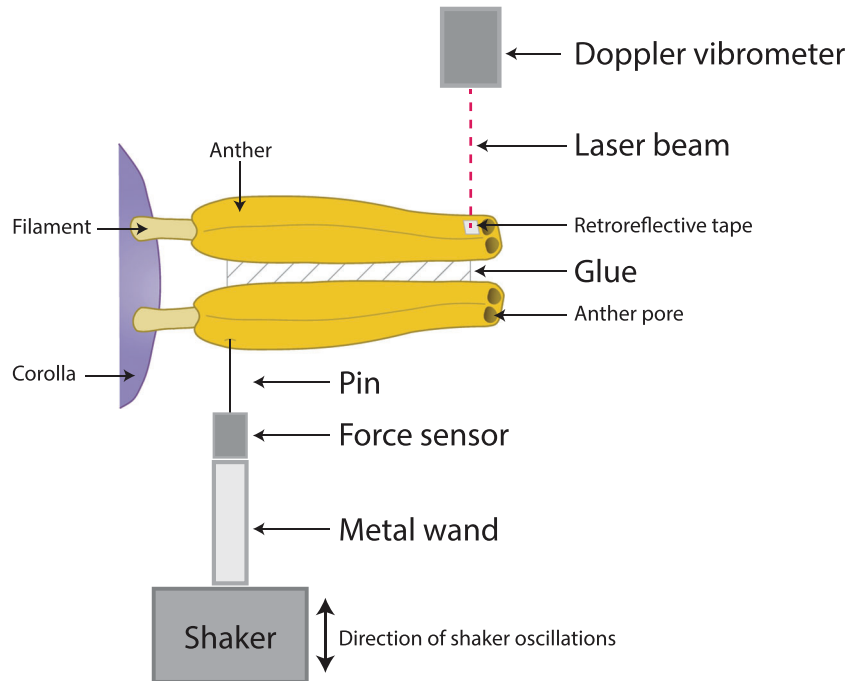
Figure 2. Diagram of the experimental setup (for details, see *Methods*). Diagram not to scale.

as needed with Tomorite Concentrated Tomato Food (Levington, Surrey, UK).

SIGNAL GENERATION

To mimic a vibration produced by bees during buzz pollination, we synthesized a pure tone at 300 Hz of 2 s in duration with a 50-ms fade-in and fade-out feature using *seewave* (Sueur et al. 2008) and saved it as a mono WAV file at a sampling rate of 44.1 kHz. The 50-ms fade-in and fade-out features in the synthesized signal were introduced to avoid amplitude spikes in the playback equipment caused by a rapid voltage change. The frequency, amplitude, and duration of the synthetic buzz were carefully chosen to capture the type of pollination buzzes observed in medium to large buzz pollinating bees (Burkart et al. 2011; De Luca and Vallejo-Marin 2013; Arroyo-Correa et al. 2019; De Luca et al. 2019; Pritchard and Vallejo-Marín 2020; Rosi-Denadai et al. 2020; Vallejo-Marín 2022). The choice of a single frequency, duration, and amplitude enabled us to focus on the comparison between the two contrasting anther architectures studied here while controlling for buzz type. Although spectral properties of bee vibrations, such as their fundamental frequency, vary between bee species, between individuals of the same species, and even between buzzes by the same bee (Burkart et al. 2011; Arroyo-Correa et al. 2019; De Luca et al. 2019; Switzer et al. 2019; Bochorny et al. 2021), we selected a single test frequency based on previous empirical work in *Solanum*, which has established that, within the range of frequencies produced by bees

($\sim$100–400 Hz), frequency has a relatively minor contribution to pollen release compared to the amplitude and duration of the buzz (De Luca et al. 2013; Rosi-Denadai et al. 2020; see also the theoretical model of Hansen et al. 2021). Future work might benefit from exploring the effect of other combinations of parameters on pollen release and vibration transmission (principally amplitude and duration that are linked to pollen release [De Luca et al. 2013; Vallejo-Marín 2019; Rosi-Denadai et al. 2020], but also other potential sources of variation including frequency, harmonic structure, different modes of the bee holding the flower while buzzing, humidity variation, etc.), but this lies beyond the scope of our study.

VIBRATION SYSTEM

We built a vibration system to generate and apply vibrations to experimental flowers (Fig. 2). A permanent magnetic shaker (LDS-V210, Brüel & Kjær, Nærum, Denmark) attached to a linear power amplifier (LDS-LPA100, Brüel & Kjær) that received the signal played back in the computer was used to generate the vibration. An M4, 10-cm stainless steel screw ("wand") (ACCU, Huddersfield, UK) was attached to the magnetic shaker. A miniature IPC force sensor (209C11, PCB Piezotronics) was placed at the end of the wand. The system was attached to the flower using an entomological pin "00" of 0.30 mm in diameter (Austerlitz, Entomoravia, Czech Republic), cut 10 mm from the tip, and superglued to a head screw in the force sensor (Fig. 2).
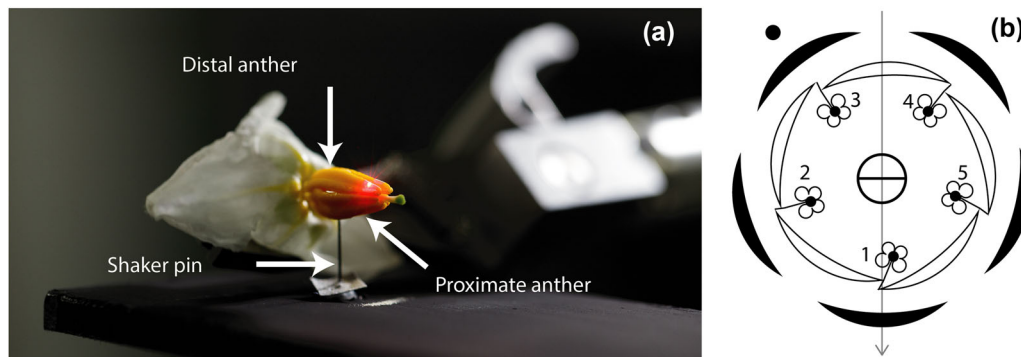
Figure 3. (a) Close up of the experimental setup showing the attachment of the shaker system via an entomological pin to the proximate anther (anther 1 in panel [b]) and the laser beam of the Doppler vibrometer targeting one of the distal anthers (either anther 3 or 4 in panel [b]). (b) Floral diagram of *Solanum* showing the labeled anthers (1–5). Floral diagram modified from Robyns (1931) and Knapp (2002).

VIBRATION PLAYBACK

The synthesized signal was played back in Audacity version 3.0 (Audacity 2021) using a laptop computer (HP Elitebook) with the volume set to 70% and output to the linear amplifier. We adjusted the gain in the linear power amplifier by hand to generate approximately 80 mm/s peak velocity (∼56 mm/s, Root Mean Square [RMS] velocity) measured in a small piece of retroreflective tape at the base of the pin. The tape was kept in place after calibration. The value of peak velocity was chosen to be within the range of values observed in buzz-pollinating bumblebees (De Luca et al. 2013), and used previously in pollen release experiments (Kemp and Vallejo-Marin 2021). Calibration measurements were taken and recorded each day at the start and end of the experimental run.

EXPERIMENTAL TREATMENT

Flowers were collected in the morning from plants growing in the cabinets or, more rarely, the glasshouses and immediately transferred to a temperature- and humidity-controlled laboratory (19°C, 40% RH) for data acquisition. The age of the flower was recorded as days since anthesis (day 1 = flowered opened that day). Flowers were removed from the inflorescence by cutting at the base of the pedicel and placing them in wet floral foam (Oasis Ideal Floral Foam Maxlife, Smithers-Oasis UK Ltd, Washington, UK) on a plastic container. Flowers were measured within 1–3 hours of being removed from plant.

Once in the lab, each flower was randomly assigned to one of two treatments: (1) Free configuration: This represents the natural arrangement of the flowers. A small amount of PVA glue was applied as a sham treatment to the outside of the anther. (2) Joined configuration: The anthers were glued together using a small amount of PVA applied along the lateral edge of each anther without blocking the pores. The treatment was applied with the help of a dissecting scope (6.7× magnification). Every flower

in the experiment experienced both treatments assigned in a random order. When the free configuration treatment was applied to a flower that had been previously glued for the joined configuration treatment, the anthers were freed using fine-tip forceps and the anthers were carefully separated from each other while leaving the glue on the anther (in some cases a small amount of glue fell off in the process of freeing the anthers).

To increase the reflectivity of the anther surface for Doppler vibrometry, we placed a small square of retroreflective tape (approximately 1—4 mm^2) onto a single anther in the adaxial side of the flower (anther 3 or 4 in Fig. 3) depending on which one presented a surface that was perpendicular to the laser beam and parallel to the axis of the vibrations produced by the shaker (Fig. 2). The tape was placed as close to the tip of the anther as possible, without blocking the pores. The tape was attached to anthers 3 or 4 (at the top of the flower). The shaker pin was inserted at the base of anther 1 (the lowest most anther, see Fig. 3). Sometimes, we used the dissecting microscope to draw a small dot made with a black marker to help placing the pin in the exact desired location. The pin made a microscopic wound in the anther. The pin was carefully pushed into the anther without going all the way through.

During the experiment, the flower was held by the pedicel using a stainless-steel micro-V clamp (VK250/M; Thorlabs Ltd., Ely, UK) on a 100-mm post (TR100/M), held in a 40-mm post holder (PH40/M), perpendicular to the ground. The post holder was screwed in an adjustable-angle mounting plate (AP180/M; Thorlabs) placed on a linear stage (M-UMR8.25; Newport Spectra-Physics Ltd, Didcot, UK) with a standard resolution micrometer (BM17.25; Newport) (see Jankauski 2020). The system was attached to a vertical translation stage (VAP10/M; Thorlabs) fixed to a 250 × 300 × 12.7 mm aluminum breadboard (MB2530/M). To reduce external vibration noise, the breadboard was placed on four sorbothane isolators (25.4 mm × 27 mm

in diameter; AV4/M) and rested on an antivibration table.

VIBRATION RECORDING

To measure the velocity of the vibrations applied and measured, we used a Doppler laser vibrometer (PDV-100, Polytec Ltd, Coventry, UK) set to 500 mm/s maximum velocity and a Low Pass Filter at 22 kHz. The force applied by the shaker was simultaneously measured using the miniature force sensor. The signals of both the laser vibrometer and the force sensor were simultaneously acquired using a two-channel NI9250 Sound and Vibration module (NI Corporation [UK] Ltd, Newbury, UK) and a USB-powered data acquisition module (cDAQ-9171, NI). The acquisition was done using custom-written software in LabView NXG 5.1 (NI). Samples were acquired at a rate of 10,240 samples per second. Data were saved in TDMS format and subsequently converted to text files using a custom program in LabView.

SIGNAL PROCESSING

For each recorded vibration, we estimated the dominant frequency (Hz) and the RMS amplitude for both the velocity (mm/s) measured in the distal anther, and the force (mN) measured in the proximate anther. The text file containing the velocity and force measurements for each vibration was processed in R version 4.0.5 (R Core Development Team 2021) using the package *seewave* (Sueur et al. 2008). In brief, we first removed the offset of the signal and used the *timer* function (threshold = 3, dmin = 1, window size = 30, no overlap) on the force channel to identify the segment of the recording to be analyzed (approximately 2 s or 20,480 samples per channel). For each channel, we then applied a high-pass filter at 20 Hz (Hanning window, window length = 520 samples) to remove background noise. The filtered signal was then used to obtain a power spectrum using the function *spec* (PSD = TRUE) with a Hanning window of 1024 samples and a frequency range of 0–2000 Hz. The RMS amplitude was calculated on the same filtered signal.

POLLEN COLLECTION

The pollen ejected through floral vibrations was collected on a plate made of black polyethylene measuring 13 cm × 5 cm × 4 mm (4083829; RS Components Ltd, Corby, UK) (see Ito et al. 2020). The plate had a hole drilled at 2 cm from one of the short edges at the midline to allow the shaker wand to go through. The surface of the plate was painted with black acrylic paint (Black 3.0, Culture Hustle, Dorset, UK) (two layers) to increase the contrast of pollen grains against the background. The polyethylene slide was positioned immediately below the flower with the aid of a micromanipulator (M330 with M3 tilting base and 2.5 kg weight; World Precision Instruments, Hitchin, UK). After the vibration was applied, the ejected, light-colored, pollen

fell on the slide and provided a good contrast against the black background. The pollen was collected from the slide using a 2-mm^3 cube of fuchsine-glycerol jelly kept at room temperature. The jelly with the collected pollen was then placed in a 1.5-mL microcentrifuge tube and stored at 4°C until pollen counting.

POLLEN COUNTING

To estimate the number of pollen grains released after experimental buzz, we used a particle counter (Multisizer 4e Coulter Counter, Indianapolis, USA). Each pollen sample (contained in a 2-mm^3 piece of fuchsin jelly in a vial) was suspended in 1 mL distilled water by heating it at 80°C for at least 30 min, then shaking the vial vigorously with the help of an electric shaker until the vial content looked homogeneous. Prior to counting with the particle counter, the vial contents were added to 19 mL 0.9% NaCl solution, for a total volume of approximately 20 mL. For each sample, the amount of pollen was counted in four 1-mL subsamples. Only particles within the size range of 15–30 µm were included in downstream analysis. Although the size of viable pollen grains within the studied species is much less variable and averaged around 24–25 µm (Fig. S1), using a broader particle size range allowed us to also include inviable pollen grains, which were considerable smaller. In total, the particle analysis counted and measured 2,291,835 particles in the 15–30 µm range (Fig. S1). We ran blank samples, containing only 0.9% NaCl solution at the beginning of every daily session and regularly between samples to ensure the equipment calibration accuracy. Finally, we summed the pollen counts for the four subsamples and multiplied by five to obtain each pollen release estimate.

STATISTICAL ANALYSIS

To analyze the effect of anther treatment (free vs. joined) on vibration RMS (root mean square) amplitude, we used generalized mixed-effects models using the package *lme4* (Bates et al. 2014) in R version 4.0.5 (R Core Development Team 2021). We fitted separate models for RMS velocity of the distal anther and for RMS force of the proximate anther. For each response variable, we started by fitting a full model with anther fusion treatment (free vs. joined), plant species, the interaction between anther treatment and plant species, sequential buzz order (first or second), and flower age (in days) as fixed effects. Plant accession, individual, and flower identity were used as random effects to yield the following model:

$$A_{RMS} \sim g + s + g \times s + n_{buzz} + a + (1|i_{accession}) + (1|i_{plant}) + (1|i_{flower}),$$

where A_{RMS} is vibration RMS amplitude (either velocity or force), g is anther fusion treatment, s is plant species, n_{buzz} is sequential buzz order, a is flower age, and $i_{accession}$, i_{plant}, and i_{flower}

are indices corresponding to accession, individual, and flower identity, respectively. For distal anther velocity, the full model yielded a singular fit and thus we reduced model complexity by removing the plant accession random effect ($i_{accession}$). This simplified model yielded qualitatively identical results to the full model (results not shown) while avoiding the fit singularity. For proximate anther velocity, the full model also yielded a singular fit, and thus we sequentially removed the random effects of plant accession and plant identity ($i_{accession}$, i_{plant}). The simpler model also yielded qualitatively identical results (coefficients and statistical significance) to the full model (results not shown). No overdispersion of the residuals of the final models was detected with the statistical package *DHARMa* (Hartig 2021).

To test for the effect of anther configuration on pollen release, we also fitted a generalized mixed-effects model using the number of pollen grains removed per buzz as the response variable. The response variable was square root transformed to improve the distribution of the residuals. The fitted model was as follows:

$$\sqrt{r} \sim g + s + g \times s + n_{buzz} + a + (1|i_{accession}) + (1|i_{plant}) + (1|i_{flower}),$$

where r is number of pollen grains removed, and other variables are as previously defined. No singular fit was detected in this case and the full model was used in the final analysis. No overdispersion of the residuals was detected with the statistical package *DHARMa* (Hartig 2021). Statistical significance of fixed effects (*P*-values) for all final models were obtained using Type III analysis of variance and Satterthwaite's estimation of degrees of freedom implemented in the package *lmerTest* (Kuznetsova et al. 2017). Given that we detected species × treatment interactions (see *Results*), we calculated the estimated marginal means with treatment nested within species using the fitted mixed-effects model in the *R* package *emmeans* (Lenth 2021). Statistical significance of the linear contrast (free – joined) was obtained using a Kenward–Roger approximation of degrees of freedom.

Results

We found a statistically significant effect of anther fusion treatment, which depended on plant species, on both the velocity of the distal anther and on the force measured in the proximate anther (treatment × species interaction; Table 2; Fig. 4). For distal anther velocity, we found that anther fusion increased the RMS velocity achieved by distal anthers compared to the free anther treatment (Fig. 4). The effect of treatment on RMS (root mean square) velocity was significant for all within species comparisons (estimated marginal means contrasts, $P < 0.0001$)

Table 2. Statistical analysis of the effect of anther fusion treatment (free vs. joined), buzz order (first or second), and flower age on the RMS amplitude velocity measured in the distal anther, and RMS amplitude force experienced by the proximate anther in three *Solanum* species. Model estimates were obtained from a linear mixed-effects model with individual and/or flower identity as random effects (see *Methods*). Statistical significance (*P*-values) of the fixed effects was calculated with a Type III analysis of variance. Significant effects (*P*-value < 0.05) are shown in bold. The reference level used for coefficient estimation is *S. pyracanthos*, free stamen configuration.

| Variable	Model Coefficient	Velocity (mm/s; Distal Anther) Estimate	SE	P-value	Force (mN; Proximate Anther) Estimate	SE	P-value
Treatment	Intercept	63.456	12.122		117.397	1.522	**<0.001**
	Joined	63.273	8.582	**<0.001**	6.925	0.795	**<0.001**
Species	*S. elaeagnifolium*	−48.609	11.553		−1.014	1.371	
	S. sisymbriifolium	−40.225	10.297	0.073		1.263	**<0.001**
Species × Treatment	*S. elaeagnifolium* × joined	46.774	12.406			1.149	
	S. sisymbriifolium × joined	53.146	10.969	**<0.001**	−4.384	1.016	**<0.001**
Buzz order	Order	2.862	4.630	0.537		0.431	0.663
Flower age	Days	−3.739	5.077	0.463		0.823	0.481
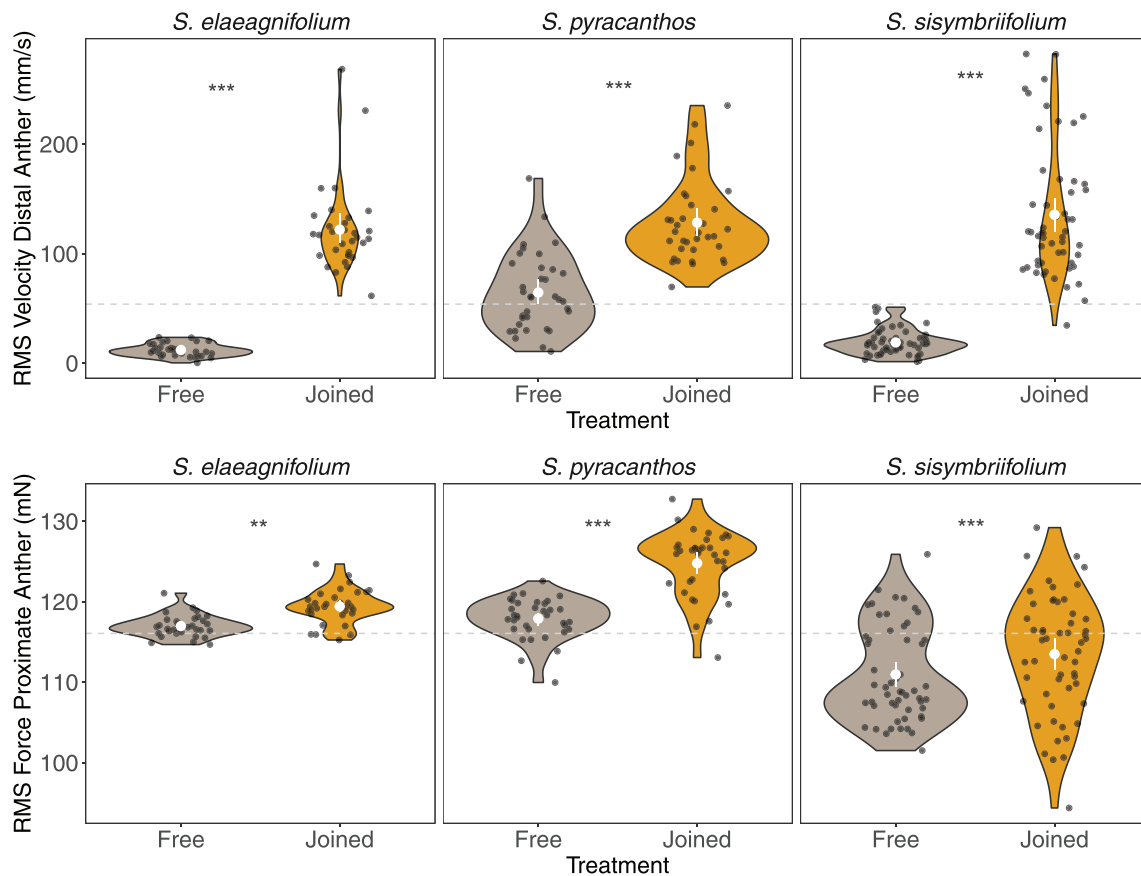
Figure 4. Vibration properties measured in anthers of three species of *Solanum* with experimentally joined anther cones ("Joined"; golden symbols) and without ("Free"; gray symbols). The "Joined" anther cones are created by gluing anthers together with water-based polyvinyl acetate glue (PVA). The bottom row shows the vibration force (root mean square, RMS force in mN) measured in the anther to which the mechanical vibrations were applied (proximate anther). The top row shows the vibration velocity (RMS velocity in mm/s) in a different anther in the opposite side of the cone (distal anther). As a reference, the experiment-wide median RMS values of the vibration velocity (53.85 mm/s) and force (116.05 mN) of the mechanical shaker measured both before the flower was attached to the system, and after it was removed, are shown with a dashed line. Dark circles represent observed data, with random noise added in the *x*-axis to facilitate visualization. The white symbols inside the violin plots indicate the mean and 95% confidence interval of the mean calculated using 1000 bootstrap replicates. Asterisks indicate statistical significance of within-species comparisons between treatments (marginal means contrasts): ***$P < 0.001$; **$P < 0.005$.

but the marginal means contrast was 73–83% higher for *S. elaeagnifolium* (110.0 ± 8.93 mm/s) and *S. sisymbriifolium* (116.4 ± 6.88 mm/s) than for *S. pyracanthos* (63.3 ± 8.58 mm/s) (Fig. 4). For both *S. elaeagnifolium* and *S. sisymbriifolium*, the RMS velocity at the tip of the distal anther in the free treatment was lower than the input RMS velocity measured in the shaker, whereas the anther velocity in the joined treatment was higher than the input velocity for all species (Fig. 5). For the force measured in the proximate anther, we also found a species-dependent effect of treatment (Table 2). All species experienced a higher force in the proximate anther in the joined treatment (estimated marginal means contrasts, $P < 0.005$), although the magnitude

of this difference varied across species (marginal means difference = 2.43 ± 0.827 mN, 2.54 ± 0.637 mN, 6.93 ± 0.795 mN, for *S. elaeagnifolium*, *S. sisymbriifolium*, and *S. pyracanthos*, respectively) (Fig. 4). In *S. elaeagnifolium* and *S. pyracanthos*, the force measured in the proximate anther was generally higher than the input force measured in the shaker before loading the flower, but in *S. sisymbriifolium* RMS force in the proximate anther varied more from lower to higher compared to the one measured before loading (Fig. 5). Neither the order in which the buzzes were applied and measured, nor flower age, had a significant effect on distal anther velocity or measured force in proximate anthers (Table 2).
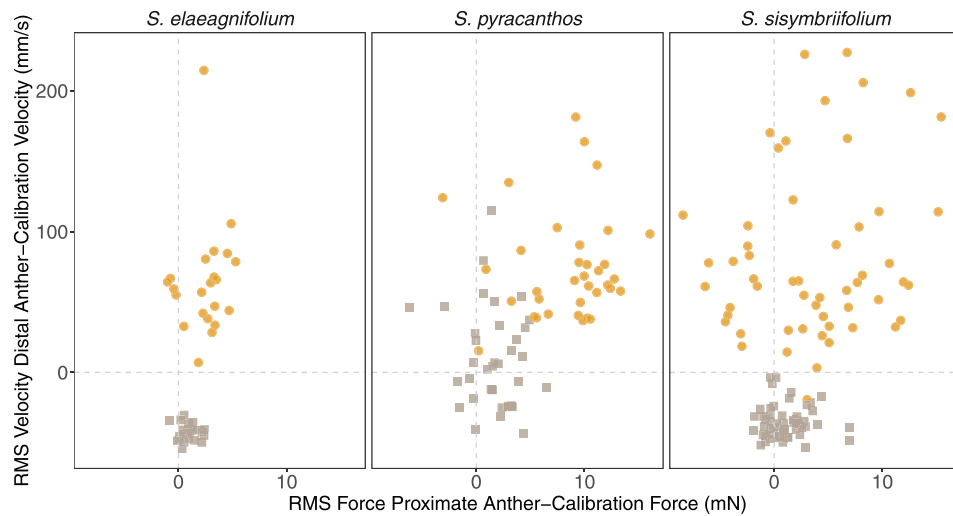
Figure 5. Relationship between RMS force measured in the anther to which mechanical vibrations are applied (proximate anther, *x*-axis) and RMS velocity of an anther located in the opposite side of the anther cone (distal anther, *y*-axis). RMS values are shown relative to the average daily values of RMS force and velocity measured during calibration of the mechanical shaker system. Symbol shape and color indicate the experimental treatment: "Joined" is shown in golden circles, and "Free" in gray squares. Within each category, each symbol indicates a different flower. All flower received both treatments in random order.

Table 3. Statistical analysis of the effect of anther fusion treatment (free vs. joined), buzz order (first or second), and flower age on number of pollen grains released after single buzzes in flowers from three *Solanum* species. Model estimates were obtained from a linear mixed-effects model with accession, individual, and flower identity as random effects using a square-root transformation of pollen grains removed. Statistical significance (*P*-values) of the fixed effects was calculated with a Type III analysis of variance. Significant effects (*P*-value < 0.05) are shown in bold. The reference level used for coefficient estimation is *S. pyracanthos*, free stamen configuration.

Variable	Model Coefficient	Estimate	SE	*P*-value
	Intercept	76.152	20.960	
Treatment				**<0.001**
	Joined	−12.332	8.915	
Species				0.609
	S. elaeagnifolium	−35.432	23.895	
	S. sisymbriifolium	−47.562	22.725	
Species × Treatment				**<0.001**
	S. elaeagnifolium × joined	60.545	12.966	
	S. sisymbriifolium × joined	50.645	11.422	
Buzz order	Order	−4.269	4.842	0.379
Flower age	Days	18.777	6.165	**0.003**

Floral vibrations removed on average 9531 ± 679 pollen grains per buzz (mean ± SE; range 55–59,665, *n* = 240). We found a significant effect of anther treatment on pollen release that depended on plant species (species × treatment interaction; Table 3). For *S. elaeagnifolium* and *S. sisymbriifolium*, more pollen (1500–2300 more pollen grains; square-root transformed marginal means estimates = 48.2 ± 9.38 and 38.3 ± 7.18, respectively; *P* < 0.0001) was released in the

joined than in the free anther treatment (Fig. 6). Conversely, the average number of pollen grains released in *S. pyracanthos* was not statistically different between free and joined treatments (estimated marginal means contrast 12.3 ± 8.91 pollen$^{1/2}$, *P* = 0.169; Fig. 6). The order in which the buzzes were applied and measured did not affect pollen release, but older flowers released significantly more pollen grains (Table 3).
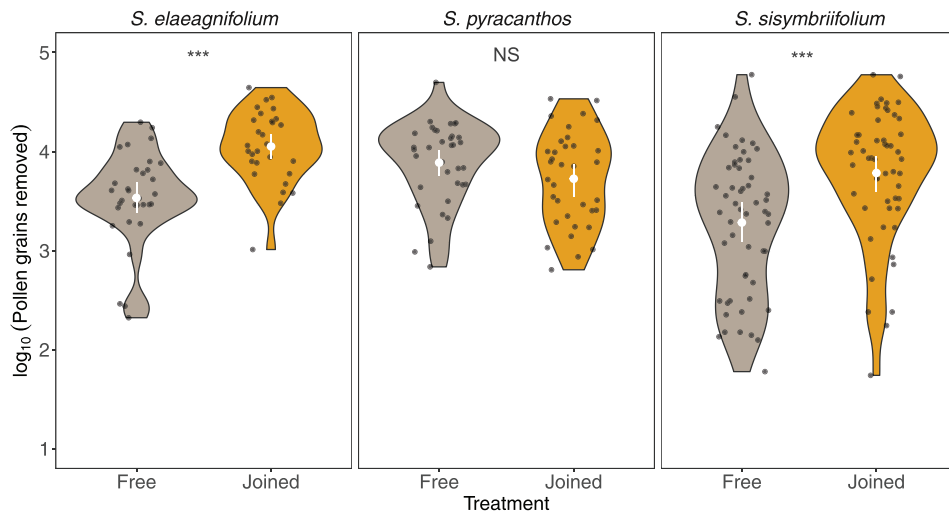
Figure 6. Effect of experimental manipulation of the anther cone on the number of pollen grains removed during a single buzz in three species of buzz-pollinated *Solanum* species. Dark circles represent observed data, with random noise added in the *x*-axis to facilitate visualization. The white symbols inside the violin plots indicate the mean and 95% confidence interval of the mean calculated using 1000 bootstrap replicates. Comparison of the effect of treatment (marginal means contrast): NS = $P > 0.05$, ***$P < 0.001$.

Discussion

In this study, we set out to address how different anther architectures, specifically the presence or absence of joined anther cones in buzz-pollinated flowers, affect patterns of vibration transmission and pollen release. Our results show that when applying vibrations to a focal (proximate) anther, the vibration velocity experienced in other (distal) anthers is significantly higher in flowers with joined anther cones, compared to those with free anthers. This result is consistent with our hypothesis that joined anther cones enable more effective transmission of applied vibrations from proximate to distal anthers via both the filament and the anther–anther pathways. Importantly, this difference in vibration transmission across anthers translates to functional differences in pollen release. In two species that naturally have loosely held, and sometimes sprawling anther architectures (*S. elaeagnifolium* and *S. sisymbriifolium*), experimental anther fusion results in more pollen released per buzz. In another species that naturally has nonjoined but tightly held anthers forming a cone (*S. pyracanthos*), experimental anther fusion did not increase pollen release. Anther fusion thus increases pollen release more strongly in species with loosely held, sprawling anthers, than in those in which anthers form a nonjoined but tightly held cone. Our study suggests that anther architecture and the evolution of joined anther cones might serve to influence the rate of pollen released across the flower following vibrations applied to individual anthers. Future work will be required to determine how anther architecture affects other vibrational properties of flowers, including their natural frequency, which has thus far been studied only in individual anthers detached from

flowers (King and Buchmann 1995, 1996; Nunes et al. 2021; Jankauski et al. 2022).

CONVERGENT EVOLUTION OF JOINED ANTHER CONES

The repeated and independent evolution of joined anther cones within the genus *Solanum* and its close relatives represents an example of convergent morphological evolution, sometimes involving different genetic, physiological, and morphological pathways (Glover et al. 2004; Davis 2019). Anther morphology and architecture within *Solanum* is often thought to be relatively conserved (Faegri 1986), although morphological and functional modification of the androecium within the genus is well known (Knapp 2002; Bohs et al. 2007; Stern et al. 2010; Vallejo-Marin et al. 2014). For example, differentiation of stamens within a flower into two or more types (heteranthery) has occurred independently multiple times within *Solanum* (Bohs et al. 2007). Yet experimental tests of the functional consequences of heteranthery in *Solanum* have only been carried out in a few species (Vallejo-Marin et al. 2009; Papaj et al. 2017). Our results provide experimental evidence that the repeated evolution of another form of stamen modification, the evolution of joined anther cones, may reflect functional convergence in *Solanum*. Further work across species (or populations) with and without naturally joined anther cones will help establishing the extent to which phylogenetic patterns of convergent morphological evolution translate to convergence on similar functions both in *Solanum* and in other plant families in which buzz-pollinated flowers

have convergently evolved joined anther cones (Endress 1996a; Holstein and Gottschling 2018).

FUNCTIONAL CONSEQUENCES OF JOINED ANTHER CONES

The evolution of joined anther cones is likely to incur different costs and benefits for flower function depending on interactions with floral visitors. Given that regardless of anther architecture, both focal and nonfocal anthers release pollen upon vibrations (e.g., Nevard et al. 2021, and the present study), joined anther cones might reduce pollen wastage by directing more pollen onto the bee's body (Glover et al. 2004). We call this the reduced pollen wastage hypothesis. Reducing the amount of pollen grains that misses the body of floral visitors should increase pollination success. At the same time, this anther architecture may involve a trade-off if bees can also benefit from joined anther cones by capturing a greater proportion of pollen that is released upon vibrating. For example, the stereotypical C-shape posture that bees take during the production of floral vibrations (De Luca and Vallejo-Marin 2013) should favor the receipt of pollen grains in the ventral region, where bees are generally capable of grooming and harvesting pollen grains (Vallejo-Marin et al. 2009; Huang et al. 2015; Koch et al. 2017; Tong et al. 2019). Reduced pollen wastage could also be achieved in flowers with loosely held anthers if the visiting bee can gather together all stamens using its legs and mandibles (M. Mayberry, D. McCart, J. Burrow, T.L. Ashman, and A. Russell, unpubl. data). Bees that are relatively large compared to the flower they visit should be capable of such manipulation, although quantitative evidence of this behavior remains scarce. At the same time, the evolution of loosely held anthers might be favored when buzzing bees can remove pollen from only one or a few anthers but only infrequently contact the stigma, such as when the bees are relatively small compared to the flower (Li et al. 2015; Solis-Montero and Vallejo-Marin 2017; Telles et al. 2020; Mesquita-Neto et al. 2021). In this context, loosely held anthers that reduce vibrations being transmitted to nonfocal anthers (as shown in our study) would simultaneously reduce pollen wastage and pollen theft. We call this the reduced costs of pollen thieves hypothesis. The hypotheses of reduced pollen wastage and reduced costs of pollen thieves highlight how the potential benefits of fused anther cones depend on ecological context, namely, the presence and abundance of floral visitors differing in size and behavior. For example, in ecological communities dominated by large bee pollinators capable of embracing all loosely held anthers and intercepting most of the ejected pollen with their bodies (e.g., carpenter bees), the benefits of reducing pollen wastage to the plant (when pollen grains miss the visitor's body) may be relatively minor. Conversely, the conditions for the reduced cost of pollen thieves hypothesis may prevail in communities where smaller bees acting as pollen thieves are dominant (Mesquita-Neto et al. 2018).

Additionally, the evolution of joined anther cones may increase the precision of pollen placement on specific parts of the pollinator's body, which could increase the likelihood of stigma contact (unimodal pollen deposition hypothesis). During buzz pollination, anther cones are expected to interact with the bee's ventral side depositing pollen in a single region (unimodal), making the location of pollen placement and pick-up relatively predictable. At the same time, unimodal pollen deposition could involve a trade-off, if the pollen were thus more readily groomed into the bee's pollen baskets (Russell et al. 2021). Accordingly, the evolution of loosely held anthers could be favored if pollen were thereby more frequently deposited on hard-to-groom "safe sites" on the bee's body. The presence of loosely held anthers may also facilitate the evolution of anther specialization within a flower, if different sets of loose anthers consistently deposit pollen on different parts of the bee's body. This preliminary division of labor may facilitate the evolution of anther morphology that improves the effectiveness of the division of labor, such as heteranthery, which commonly occurs in buzz pollinated plants (Vallejo-Marin et al. 2010; Barrett 2021). Division of labor in heterantherous species is achieved by two or more types of morphologically distinct stamens that release and deposit pollen on distinct parts of the pollinator's body, one of which is more effectively groomed by floral visitors (feeding anthers) and another that is more likely to contact the stigma of other conspecific flowers (pollinating anthers) (Luo et al. 2008; Vallejo-Marin et al. 2009; Papaj et al. 2017; da Silva Saab et al. 2021). In heterantherous flowers, pollen release and deposition are thus expected to have a bimodal (or multimodal if more than two stamen types) distribution on the pollinator's body, and such distribution is incompatible with joined anther cones.

Finally, a nonmutually exclusive hypothesis, for which our results provide direct empirical support, is that joined anther cones increase the transmission of vibrations across the stamens and, in some case, result in higher rates of pollen released per buzz (increased pollen release hypothesis). Our experiments across three *Solanum* species with slightly different anther architectures show that in all cases, joined anther cones significantly increase the vibration amplitude (RMS velocity) transmitted to nonfocal anthers showing an immediate consequence of joined anther cones. However, our experiments also show that the extent to which experimental fusion of anther cones influence pollen release is contingent on species-specific characteristics. Pollen release was increased in the two species that naturally have loosely arranged anther architectures (*S. elaeagnifolium* and *S. sisymbriifolium*), and in which the experimental treatment notably increases the extent to which anthers contact each other (the anther–anther vibration transmission pathway). An increase in pollen

release through anther fusion is not observed in the Malagasy species *S. pyracanthos*, in which anthers are closely held together since the beginning of anthesis and throughout the flower's life. Although vibration amplitude in joined anthers of *S. pyracanthos* increases, we found no effect on pollen release. This might be because, despite being nonjoined by either trichomes or bioadhesives, the closely held androecium of *S. pyracanthos* is sufficient to transmit strong enough vibrations across all anthers to maximize pollen release rate. Pollen release rate in this case might be limited not by vibration amplitude, but by other factors such as the size of the apical pore from which pollen can come out during buzzing, and the amount of freely available pollen inside the anther locules, which in part is determined by flower age (Harder and Barclay 1994; Kemp and Vallejo-Marin 2021).

The four hypotheses mentioned above are not an exhaustive list or mutually exclusive, and they could act in concert, for example, by simultaneously reducing pollen wastage and increasing pollen release rates. Other consequences of free anthers could include lengthening the amount of time that a visitor spends in a flower, due to having to separately manipulate anthers, which in some cases might increase pollen deposition on the stigma, including self-pollen deposition. However, a common feature of these hypotheses is their dependence on specific ecological factors, particularly the morphological and behavioral characteristics of floral visitors. Evaluating the relative value of these hypotheses in explaining the evolution of joined anther cones, therefore, requires explicitly considering the interaction of buzz pollinated plants and their wild bee pollinators.

CONFLICT OF INTEREST
The authors declare no conflict of interest.

DATA ARCHIVING
The vibration and pollen data are available at https://doi.org/10.5061/dryad.s1rn8pk9p.

REFERENCES
Armbruster, W. S., J. Lee, M. E. Edwards, and B. G. Baldwin. 2013. Floral paedomorphy leads to secondary specialization in pollination of Madagascar *Dalechampia* (Euphorbiaceae). Evolution 67:1196–1203.

Arroyo-Correa, B., C. E. Beattie, and M. Vallejo-Marin. 2019. Bee and floral traits affect the characteristics of the vibrations experienced by flowers during buzz-pollination. J. Exp. Biol. 222:jeb198176.

Audacity. 2021. Audacity (ver. 3.0.2). Available via https://www.audacityteam.org.

Barrett, S. C. 2021. Heteranthery. Curr. Biol. 31:R774–R776.

Bates, D., M. Maechler, and B. Bolker. 2014. lme4: linear mixed-effects models using Eigen and S4_. R package version 1.1-7. Available via http://CRAN.R-project.org/package=lme4.

Bochorny, T., L. F. Bacci, A. S. Dellinger, F. A. Michelangeli, R. Goldenberg, and V. L. G. Brito. 2021. Connective appendages in *Huberia bradeana* (Melastomataceae) affect pollen release during buzz pollination. Plant Biol. 23:556–563.

Bohs, L., T. Weese, N. Myers, V. Lefgren, N. Thomas, A.v. Wagenen, and S. Stern. 2007. Zygomorphy and heteranthery in Solanum in a phylogenetic context. Acta Hort. 745:201–224.

Brito, V. L. G., C. E. P. Nunes, C. R. Resende, F. Montealegre-Zapata, and M. Vallejo-Marín. 2020. Biomechanical properties of a buzz-pollinated flower. R. Soc. Open Sci. 7:201010.

Buchmann, S. L. 1983. Buzz pollination in angiosperms. Pp. 73–113 *in* C. E. Jones and R. J. Little, eds. Handbook of experimental pollination biology. Van Nostrand Reinhold, New York.

Buchmann, S. L., and J. H. Cane. 1989. Bees assess pollen returns while sonicating *Solanum* flowers. Oecologia 81:289–294.

Buchmann, S. L., and J. P. Hurley. 1978. Biophysical model for buzz pollination in Angiosperms. J. Theor. Biol. 72:639–657.

Buchmann, S. L., C. E. Jones, and L. J. Colin. 1977. Vibratile pollination of *Solanum douglasii* and *Solanum xanti* (Solanaceae) in Southern California USA. Wasmann Journal of Biology 35:1-25.

Burkart, A., K. Lunau, and C. Schlindwein. 2011. Comparative bioacoustical studies on flight and buzzing of neotropical bees. Journal of Pollination Ecology 6:118-224.

D'Arcy, W. G. 1992. Solanaceae of Madagascar: form and geography. Annals of the Missouri Botanical Garden 79:29-45.

Darwin, C. 1877. The different forms of flowers on plants of the same species. J. Murray, Lond.

da Silva Saab, G., V. de Freitas Mansano, A. Nogueira, I. C. Maia, P. J. Bergamo, and J. V. Paulino. 2021. A sophisticated case of division of labour in the trimorphic stamens of the *Cassia fistula* (Leguminosae) flower. AoB Plants 13:plab054.

Davis, G. V. 2019. The evolution of male form and function in nightshade flowers. Doctoral thesis. University of Cambridge, Cambridge, U.K.

De Luca, P. A., and M. Vallejo-Marin. 2013. What's the 'buzz' about? The ecology and evolutionary significance of buzz-pollination. Current Opinion in Plant Biology 16:429-435.

De Luca, P. A., L. F. Bussiere, D. Souto-Vilaros, D. Goulson, A. C. Mason, and M. Vallejo-Marín. 2013. Variability in bumblebee pollination buzzes affects the quantity of pollen released from flowers. Oecologia 172:805-816.

De Luca, P. A., S. Buchmann, C. Galen, A. C. Mason, and M. Vallejo-Marin. 2019. Does body size predict the buzz-pollination frequencies used by bees? Ecology and Evolution 9:4875-4887.

Dean, E., J. Poore, M. A. Anguiano-Constante, M. H. Nee, H. Kang, T. Starbuck, A. Rodrígues, and M. Conner. 2020. The genus *Lycianthes* (Solanaceae, Capsiceae) in Mexico and Guatemala. PhytoKeys 168:1–333.

Endress, P. K. 1996a. Diversity and evolutionary trends in angiosperm anthers. Pp. 92–110 *in* W. G. D'Arcy, and R. C. Keating, eds. The anther: form, function and phylogeny. Cambridge Univ. Press, Cambridge, U.K.

———. 1996b. Homoplasy in Angiosperm flowers. Pp. 303–325 *in* S. J. Sanderson, and L. Hufford, eds. Homoplasy - the recurrence of similarity in evolution. San Diego Academic Press, San Diego, CA.

Faegri, K. 1986. The solanoid flower. Transactions of the Botanical Society of Edinburgh 45:51-59.

Falcão, B. F., C. Schlindwein, and J. R. Stehmann. 2016. Pollen release mechanisms and androecium structure in *Solanum* (Solanaceae): does anther morphology predict pollination strategy? Flora 224:211-217.

Glover, B. J., S. Bunnewell, and C. Martin. 2004. Convergent evolution within the genus *Solanum*: the specialised anther cone develops through alternative pathways. Gene 331:1-7.

Hansen, M., G. C. Lanes, V. L. Brito, and E. D. Leonel. 2021. Investigation of pollen release by poricidal anthers using mathematical billiards. Physical Review E 104:034409.

Harder, L. D., and M. R. Barclay. 1994. The functional significance of poricidal anthers and buzz pollination: controlled pollen removal from *Dodecatheon*. Functional Ecology 8:509-517.

Hartig, F. 2021. DHARMa: residual diagnostics for hierarchical (multi-level /mixed) regression models. R package.

Holstein, N., and M. Gottschling. 2018. Flowers of *Halgania* (Ehretiaceae, Boraginales) are set up for being buzzed and the role of intertwining anther trichomes. Flora 240:7-15.

Huang, Z.-H., H.-L. Liu, and S.-Q. Huang. 2015. Interspecific pollen transfer between two coflowering species was minimized by bumblebee fidelity and differential pollen placement on the bumblebee body. J Plant Ecol 8:109-115.

Ito, S., H. Rajabi, and S. N. Gorb. 2020. A ballistic pollen dispersal strategy hidden in stylar oscillation. bioRxiv. https://doi.org/10.1101/2020.01.27.920710.

Jankauski, M., R. Ferguson, A. Russell, and S. Buchmann. 2022. Structural dynamics of real and modeled *Solanum* stamens: implications for pollen ejection by buzzing bees. J. R. Soc. Interface 19:20220040.

Jankauski, M. A. 2020. Measuring the frequency response of the honeybee thorax. Bioinspiration & Biomimetics 15:046002.

Kemp, J. E., and M. Vallejo-Marin. 2021. Pollen dispensing schedules in buzz-pollinated plants: experimental comparison of species with contrasting floral morphologies. American Journal of Botany 108:1-13.

———., and ———. 1995. Bumble bee-initiated vibration release mechanism of *Rhododendron* pollen. American Journal of Botany 82:1407-1411.

———., and ———. 1996. Sonication dispensing of pollen from *Solanum laciniatum* flowers. Functional Ecology 10:449-456.

Knapp, S. 2002. Floral diversity and evolution in the Solanaceae. Pp. 267–297 *in* Q. C. B. Cronk, R. M. Bateman, and J. A. Hawkins, eds. Developmental genetics and plant evolution. Taylor & Francis, London.

———. 2014a. Solanaceae source: *Solanum elaeagnifolium* Cav. Available via http://solanaceaesource.org/taxonomy/term/106820/descriptions.

———. 2014b. Solanaceae source: *Solanum pyracanthos* Lam. Available via http://solanaceaesource.org/content/solanum-pyracanthos.

Koch, L., K. Lunau, and P. Wester. 2017. To be on the safe site - ungroomed spots on the bee's body and their importance for pollination. PLoS ONE 12:e0182522.

Kuznetsova, A., P. B. Brockhoff, and R. H. B. Christensen. 2017. lmerTest package: tests in linear mixed effect models. Journal of Statistical Software 82:1-26.

Lenth, R. V. 2021. emmeans: estimated marginal means, aka least-squares means. R package.

Li, J.-K., Y.-P. Song, H. Xu, Y.-W. Zhang, J.-Y. Zhu, and L.-L. Tang. 2015. High ratio of illegitimate visitation by small bees severely weakens the potential function of heteranthery. Journal of Plant Ecology 8:213-223.

Luo, Z., D. Zhang, and S. S. Renner. 2008. Why two kinds of stamens in buzz-pollinated flowers? Experimental support for Darwin's division-of-labour hypothesis. Functional Ecology 22:794-800.

Macior, L. W. 1968. Pollination adaptation in *Pedicularis groenlandica*. American Journal of Botany 55:927-932.

Mesquita-Neto, J. N., N. Blüthgen, and C. Schlindwein. 2018. Flowers with poricidal anthers and their complex interaction networks—disentangling legitimate pollinators and illegitimate visitors. Functional Ecology 32:2321-2332.

Mesquita-Neto, J. N., A. L. C. Vieira, and C. Schlindwein. 2021. Minimum size threshold of visiting bees of a buzz-pollinated plant species: consequences for pollination efficiency. American Journal of Botany 108:1006-1015.

Nevard, L., A. L. Russell, K. Foord, and M. Vallejo-Marin. 2021. Transmission of bee-like vibrations in buzz-pollinated plants with different stamen architectures. Scientific Reports 11:13541.

Nunes, C. E. P., L. Nevard, F. Montealegre-Z, and M. Vallejo-Marín. 2021. Variation in the natural frequency of stamens in six morphologically diverse, buzz-pollinated, heterantherous *Solanum* taxa and its relationship to bee vibrations. Botanical Journal of the Linnean Society 197:541–553.

Papaj, D. R., S. L. Buchmann, and A. L. Russell. 2017. Division of labor of anthers in heterantherous plants: flexibility of bee pollen collection behavior may serve to keep plants honest. Arthropod-Plant Interactions 11:307-315.

Petanidou, T., M. V. Price, J. L. Bronstein, A. Kantsa, T. Tscheulin, R. Kariyat, N. Krigas, M. C. Mescher, C. M. De Moraes, and N. M. Waser. 2018. Pollination and reproduction of an invasive plant inside and outside its ancestral range. Acta Oecologica 89:11-20.

Plebani, M., O. Imanizabayo, D. M. Hansen, and W. S. Armbruster. 2015. Pollination ecology and circadian patterns of inflorescence opening of the Madagascan climber *Dalechampia aff. bernieri* (Euphorbiaceae). Journal of Tropical Ecology 31:99-101.

Pritchard, D. J., and M. Vallejo-Marín. 2020. Floral vibrations by buzz-pollinating bees achieve higher frequency, velocity and acceleration than flight and defence vibrations. Journal of Experimental Biology 223:jeb.220541.

R Core Development Team. 2021. R: a language and environment for statistical computing. R Foundation for Statistical Computing, Vienna. http://www.R-project.org.

Ramos, A. F., S. G. Bauermann, L. A. Lopes, and A. C. P. Evaldt. 2016. Produção polínica de *Solanum sisymbriifolium* Lam. (Solanaceae) e a coleta de pólen pelas abelhas visitantes florais. Educação Ambiental em Ação 57:1-7.

Robyns, W. 1931. L'Organisation florale des solanacées zygomorphes. M. Lamertin, Brussels, Belgium.

Rosi-Denadai, C. A., P. C. S. Araujo, L. A. O. Campos, L. Cosme, Jr., and R. N. C. Guedes. 2020. Buzz-pollination in Neotropical bees: genus-dependent frequencies and lack of optimal frequency for pollen release. Insect Sci 27:133-142.

Russell, A. L., R. E. Golden, A. S. Leonard, and D. R. Papaj. 2016. Bees learn preferences for plant species that offer only pollen as a reward. Behavioral Ecology 27:731-740.

Russell, A. L., A. M. Fetters, E. I. James, and T.-L. Ashman. 2021. Pollinator effectiveness is affected by intraindividual behavioral variation. Oecologia 197:189-200.

Sarkinen, T., L. Bohs, R. G. Olmstead, and S. Knapp. 2013. A phylogenetic framework for evolutionary study of the nightshades (Solanaceae): a dated 1000-tip tree. BMC Evolutionary Biology 13:214.

Solis-Montero, L., and M. Vallejo-Marin. 2017. Does the morphological fit between flowers and pollinators affect pollen deposition? An experimental test in a buzz-pollinated species with anther dimorphism. Ecology and Evolution 7:2706-2715.

Stern, S. R., T. Weese, and L. A. Bohs. 2010. Phylogenetic relationships in Solanum section Androceras (Solanaceae). Systematic Botany 35:885-893.

Sueur, J., T. Aubin, and C. Simonis. 2008. Seewave, a free modular tool for sound analysis and synthesis. Bioacoustics 18:213-226.

Switzer, C. M., A. L. Russell, D. R. Papaj, S. A. Combes, and R. Hopkins. 2019. Sonicating bees demonstrate flexible pollen extraction without instrumental learning. Current Zoology 65:425-436.

Telles, F. J., C. L. Klunk, F. R. d Maia, V. L. G. de Brito, and I. G. Varassin. 2020. Towards a new understanding of the division of labour in heterantherous flowers: the case of *Pterolepis glomerata* (Melastomataceae). Biological Journal of the Linnean Society 131:1-11.

Thorp, R. W., and J. R. Estes. 1975. Intrafloral behavior of bees on flowers of *Cassia fasciculata*. Journal of the Kansas Entomological Society 48:175-184.

Tong, Z.-Y., X.-P. Wang, L.-Y. Wu, and S.-Q. Huang. 2019. Nectar supplementation changes pollinator behaviour and pollination mode in *Pedicularis dichotoma*: implications for evolutionary transitions. Annals of Botany 123:373-380.

Tscheulin, T., T. Petanidou, S. G. Potts, and J. Settele. 2009. The impact of *Solanum elaeagnifolium*, an invasive plant in the Mediterranean, on the flower visitation and seed set of the native co-flowering species *Glaucium flavum*. Plant Ecology 205:77-85.

Vallejo-Marín, M. 2019. Buzz pollination: studying bee vibrations on flowers. New Phytologist 224:1068-1074.

———. 2022. How and why do bees buzz? Implications for buzz pollination. Journal of Experimental Botany 73:1080–1092.

Vallejo-Marin, M., J. S. Manson, J. D. Thomson, and S. C. H. Barrett. 2009. Division of labour within flowers: heteranthery, a floral strategy to reconcile contrasting pollen fates. Journal of Evolutionary Biology 22:828-839.

Vallejo-Marin, M., E. M. Da Silva, R. D. Sargent, and S. C. H. Barrett. 2010. Trait correlates and functional significance of heteranthery in flowering plants. New Phytologist 188:418-425.

Vallejo-Marin, M., C. Walker, P. Friston-Reilly, L. Solis-Montero, and B. Igic. 2014. Recurrent modification of floral morphology in heterantherous *Solanum* reveals a parallel shift in reproductive strategy. Philosophical Transactions of the Royal Society B-Biological Sciences 369:20130256.

Vogel, S. 1996. Christian Konrad Sprengel's theory of the flower: the cradle of floral ecology. Pp. 44–62 *in* D. G. Lloyd, and S. C. H. Barrett, eds. Floral biology. Chapman & Hall, New York.

Vorontsova, M. S., and S. Knapp. 2014. Solanaceae source: *Solanum sisymbriifolium*. Available via http://solanaceaesource.org/content/solanum-sisymbriifolium.

Associate Editor: S. Ramirez
Handling Editor: A. McAdam

Supporting Information

Additional supporting information may be found online in the Supporting Information section at the end of the article.

Supplementary Figure 1. Frequency distribution of the size of measured particles (pollen grains) in the electric particle counter as described in the Methods.